A SEMI-ANALYTICAL SOLUTION FOR THE PROPAGATION OF PURE SHEAR WAVES IN DISSIPATIVE MONOCLINIC MEDIA

J. M. Carcione and F. Cavallini

Osservatorio Geofisico Sperimentale, P.O. Box 2011 Opicina, 34016 Trieste, Italy.

Abstract

From the correspondence principle, and explicit knowledge of the frequency-domain elastic solution, we find a semi-analytical solution for anti-plane shear waves in the plane of mirror symmetry of a viscoelastic monoclinic medium. Then follows an example where dissipation is modelled by standard linear solid kernels, which describe the proper behaviour of relaxation mechanisms in real materials. As expected, the solution shows velocity anisotropy, anisotropic attenuation, and velocity dispersion.

Introduction

Anisotropy and anelasticity are relevant phenomena in the study of sedimentary formations in which oil and gas are stored. For instance, it is well known that, in cracked limestones and thin saturated sandstone layers embedded in anisotropic shales, the velocity and attenuation of the acoustic waves show important anisotropic behaviour.

Propagation in the plane of mirror symmetry of a monoclinic medium includes pure anti-plane strain motion, and is the most general situation for which pure shear waves exist at all propagation angles. (Pure shear wave propagation in hexagonal media is a degenerate case). A set of parallel fractures embedded in a transversely isotropic formation can be represented by a monoclinic medium. When the plane of mirror symmetry of the medium is vertical, the pure anti-plane strain waves are SH waves. Moreover, monoclinic media include many other cases of higher symmetry. Weak tetragonal media, strong trigonal media and orthorhombic media are subsets of the set of monoclinic media.

The 'anti-plane strain assumption', that particle velocity $\mathbf{v} = v(x,z)\,\hat{\mathbf{e}}_y$, implies that one of the shear waves has its own (decoupled) differential equation [1]. This is strictly true in the symmetry plane of a monoclinic medium. The solution for the dissipative case can be obtained by means of the correspondence principle [2. p.875]. This requires knowledge of the explicit expression for the elastic solution in the frequency domain. Then, the elastic constants can be replaced by the corresponding complex stiffnesses, and the viscoelastic solution is obtained by an inverse Fourier transform in time. This procedure is described in the next section.

The solution

In the plane of mirror symmetry of a monoclinic medium, the relevant stiffness matrix describing the propagation of the pure shear wave is [3]

$$\mathbf{c} = \begin{bmatrix} c_{44} & c_{46} \\ c_{46} & c_{66} \end{bmatrix}, \tag{1}$$

where c_{IJ}, I,J = 1,...,6 are the elastic constants. Substitution of the stress-strain relation based on (1) into Newton's equation gives [1]

$$\nabla^{\mathsf{T}} \bullet \mathbf{c} \bullet \nabla v - \rho \ddot{v} = f, \tag{1}$$

where ρ is the material density, f is the time derivative of the body force per unit volume, and $\nabla = [\partial_z, \partial_x]^{\mathsf{T}}$. The conventions are that the symbol ∂ denotes spatial differentiation, a dot above a variable denotes time differentiation, the superscript T indicates transpose, and the bullet $\bullet$ indicates the ordinary matrix product in two dimensions.

Since we consider here a homogeneous medium, equation (2) becomes

$$(c_{44}\partial_{zz} + c_{66}\partial_{xx} + 2c_{46}\partial_{xz})v - \rho\ddot{v} = f. \tag{3}$$

We show below that it is possible, by a transformation of coordinates, to transform the spatial differential operator on the l.h.s. of (3) to a pure Laplacian differential operator. In that case, equation (3) becomes

$$(\partial_{z'z'} + \partial_{x'x'})v - \rho\ddot{v} = f, \tag{4}$$

where x' and z' are the new coordinates. Considering the solution for the Green's function (i.e., the r.h.s. of (4) is a Dirac's delta function in time and space at the origin), and transforming the wave equation to the frequency domain, gives

$$(\partial_{z'z'} + \partial_{x'x'})\tilde{g} + \rho\omega^2\tilde{g} = -4\pi\delta(x')\delta(z'), \tag{5}$$

where $\tilde{g}$ is the Fourier transform of the Green's function and ω is the angular frequency. The constant -4π is introduced for convenience. The solution of (5) is [4, p.1362]

$$\tilde{g}(x', z', \omega) = -i\pi H_0^{(2)}(\sqrt{\rho}\,\omega r'), \tag{6}$$

where $H_0^{(2)}$ is the Hankel function of the second kind, and

$$r' = (x'^2 + z'^2)^{1/2} \equiv (\mathbf{x}'^{\mathsf{T}} \bullet \mathbf{x}')^{1/2}, \tag{7}$$

with $\mathbf{x}' = [z', x']^{\mathsf{T}}$. We need to compute (6) in terms of the original position vector $\mathbf{x} = [z, x]^{\mathsf{T}}$. Matrix $\mathbf{c}$ may be decomposed as $\mathbf{c} = \mathbf{A} \bullet \Lambda \bullet \mathbf{A}^{\mathsf{T}}$, where Λ is the diagonal matrix of the eigenvalues, and $\mathbf{A}$ is the matrix of the normalized eigenvectors. Thus, the Laplacian operator in (2) becomes

$$\nabla^{\mathsf{T}} \bullet \mathbf{c} \bullet \nabla = \nabla^{\mathsf{T}} \bullet \mathbf{A} \bullet \Lambda \bullet \mathbf{A}^{\mathsf{T}} \bullet \nabla = \nabla^{\mathsf{T}} \bullet \mathbf{A} \bullet \Omega \bullet \Omega \bullet \mathbf{A}^{\mathsf{T}} \bullet \nabla = \nabla'^{\mathsf{T}} \bullet \nabla', \tag{8}$$

where $\Lambda = \Omega^2$, and

$$\nabla' = \Omega \bullet \mathbf{A}^{\mathsf{T}} \bullet \nabla. \tag{9}$$

Using that Ω is diagonal and $\mathbf{A}^{\mathsf{T}} = \mathbf{A}^{-1}$, we get

$$\mathbf{x}' = \Omega^{-1} \bullet \mathbf{A}^{\mathsf{T}} \bullet \mathbf{x}. \tag{10}$$

Substituting (10) into equation (7) squared gives

$$r'^2 = \mathbf{x}^{\mathsf{T}} \bullet \mathbf{A} \bullet \Omega^{-1} \bullet \Omega^{-1} \bullet \mathbf{A}^{\mathsf{T}} \bullet \mathbf{x} = \mathbf{x}^{\mathsf{T}} \bullet \mathbf{A} \bullet \Lambda^{-1} \bullet \mathbf{A}^{\mathsf{T}} \bullet \mathbf{x}. \tag{11}$$

Since $\mathbf{A} \bullet \Lambda^{-1} \bullet \mathbf{A}^{\mathsf{T}} = \mathbf{c}^{-1}$, we finally have

$$r'^2 = \mathbf{x}^{\mathsf{T}} \bullet \mathbf{c}^{-1} \bullet \mathbf{x} = (c_{66}z^2 + c_{44}x^2 - 2c_{46}xz)/c, \tag{12}$$

where c is the determinant of $\mathbf{c}$.

Then, replacing (12) into equation (6), the elastic Green's function becomes

$$\tilde{g}(x, z, \omega) = -i\pi H_0^{(2)}\left[\omega(\mathbf{x}^{\mathsf{T}} \bullet \rho\mathbf{c}^{-1} \bullet \mathbf{x})^{1/2}\right]. \tag{13}$$

Application of the correspondence principle gives the viscoelastic Green's function

$$\tilde{g}_v(x, z, \omega) = -i\pi H_0^{(2)}\left[\omega(\mathbf{x}^{\mathsf{T}} \bullet \rho\mathbf{p}^{-1} \bullet \mathbf{x})^{1/2}\right], \tag{14}$$

where $\mathbf{p}$ is the complex, and frequency dependent, stiffness matrix. When solving the wave propagation problem with a band-limited wavelet $f(t)$, the solution is

$$\tilde{v}(\mathbf{x}, \omega) = -i\pi\tilde{f} H_0^{(2)}\left[\omega(\mathbf{x}^{\mathsf{T}} \bullet \rho\mathbf{p}^{-1} \bullet \mathbf{x})^{1/2}\right], \tag{15}$$

where $\tilde{f}$ is the Fourier transform of f. To ensure a time-domain real solution, when $\omega < 0$ we take

$$\tilde{v}(\mathbf{x}, \omega) = \tilde{v}^*(\mathbf{x}, -\omega) \tag{16}$$

where the superscript * denotes complex conjugation. Finally, the time domain solution is obtained by an inverse transform based on the Fast Fourier Transform.

An example and discussion

The information about the rheology is contained in matrix **p.** We assume that anelasticity is modelled by standard linear solid kernels, which, as is well known [2, p.856], describe

properly the relaxation function, phase velocity and attenuation properties of real solids. We consider a monoclinic medium with $p_{44} = c_{44}M^{(1)}$, $p_{66} = c_{66}M^{(2)}$ and $p_{46} = c_{46}$, where

$$M^{(m)}(\omega) = \frac{1 + i\omega\tau_\varepsilon^{(m)}}{1 + i\omega\tau_\sigma^{(m)}} , \qquad m = 1, 2 , \tag{17}$$

with $\tau_\varepsilon^{(m)}$ and $\tau_\sigma^{(m)}$ material relaxation times. The quality factors can be expressed as

$$Q^{(m)}(\omega) = Q_0^{(m)} \frac{1 + \omega^2\tau_0^{(m)2}}{2\omega\tau_0^{(m)}} , \qquad m = 1, 2 , \tag{18}$$

respectively, where

$$Q_0^{(m)} = \frac{2\tau_0^{(m)}}{\tau_\varepsilon^{(m)} - \tau_\sigma^{(m)}} , \qquad \text{and} \quad \tau_0^{(m)} = \sqrt{\tau_\varepsilon^{(m)}\,\tau_\sigma^{(m)}} . \tag{19}$$

The curve $Q^{(m)}(\omega)$ has its peak at $\omega_0^{(m)} = 1/\tau_0^{(m)}$, and the value of Q at the peak is $Q_0^{(m)}$. The low-frequency elasticities are taken as $c_{44} = 10\text{GPa}$, $c_{66} = 22.5\text{GPa}$ and $c_{46} = 5\text{GPa}$, and the density $\rho = 2500\text{kg/m}^3$. These give vertical and horizontal velocities of 2000m/s and 3000m/s, respectively. The relaxation peaks of both dissipation mechanisms are centred at $f_0 = 2\pi\tau_0^{(m)} = 25\text{Hz}$, and the peak quality factors are $Q_0^{(1)} = 20$ and $Q_0^{(2)} = 100$. It can be shown that these are the values of the quality factors along the z and x-directions, respectively.

Figure 1 represents the positions of five receivers relative to the source, which is located at the origin. The distance between the source and each receiver is 800m. Propagation of a zero-phase Ricker wavelet with central frequency of 25Hz gives the results shown in Figure 2, where the left and right pictures represent the anisotropic-elastic and anisotropic-anelastic cases, respectively. Each solution is normalized with respect to the elastic solution at receiver 3, whose positive peak has amplitude one. The time t_p refers to the position of the maximum positive peak. In first place, the different values of t_p at each receiver reveal the anisotropic character of the propagation. In fact it can be shown that, in the elastic case, the slowness curve is an ellipse whose major axis makes an angle $\theta = 0.5\text{atan}[2c_{46}/(c_{66} - c_{44})] \approx 20°$ with the z-axis [1]. Moreover, for each receiver, the anelastic pulse is faster than the elastic pulse. This velocity dispersion effect is explained by the fact that we chose (arbitrarily) the elastic case in the low frequency limit (relaxed state of the system), which has the lower velocity.

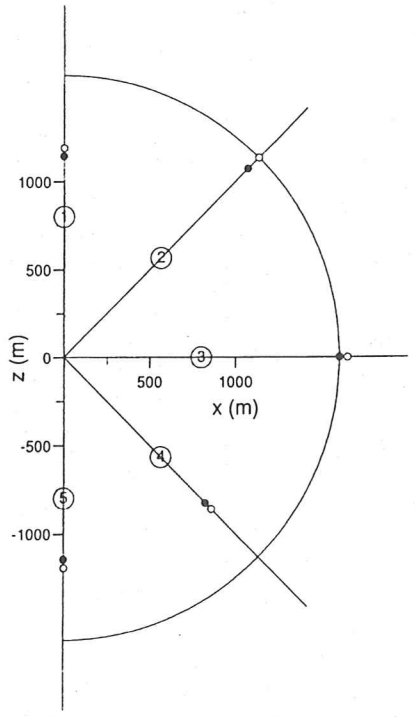

Figure 1.

Recording configuration. The receivers are numbered from 1 to 5 and are located at 800m from the origin, where the source is placed. The black and empty dots reconstruct the elastic and anelastic wavefronts from velocity information taken from Figure 2.

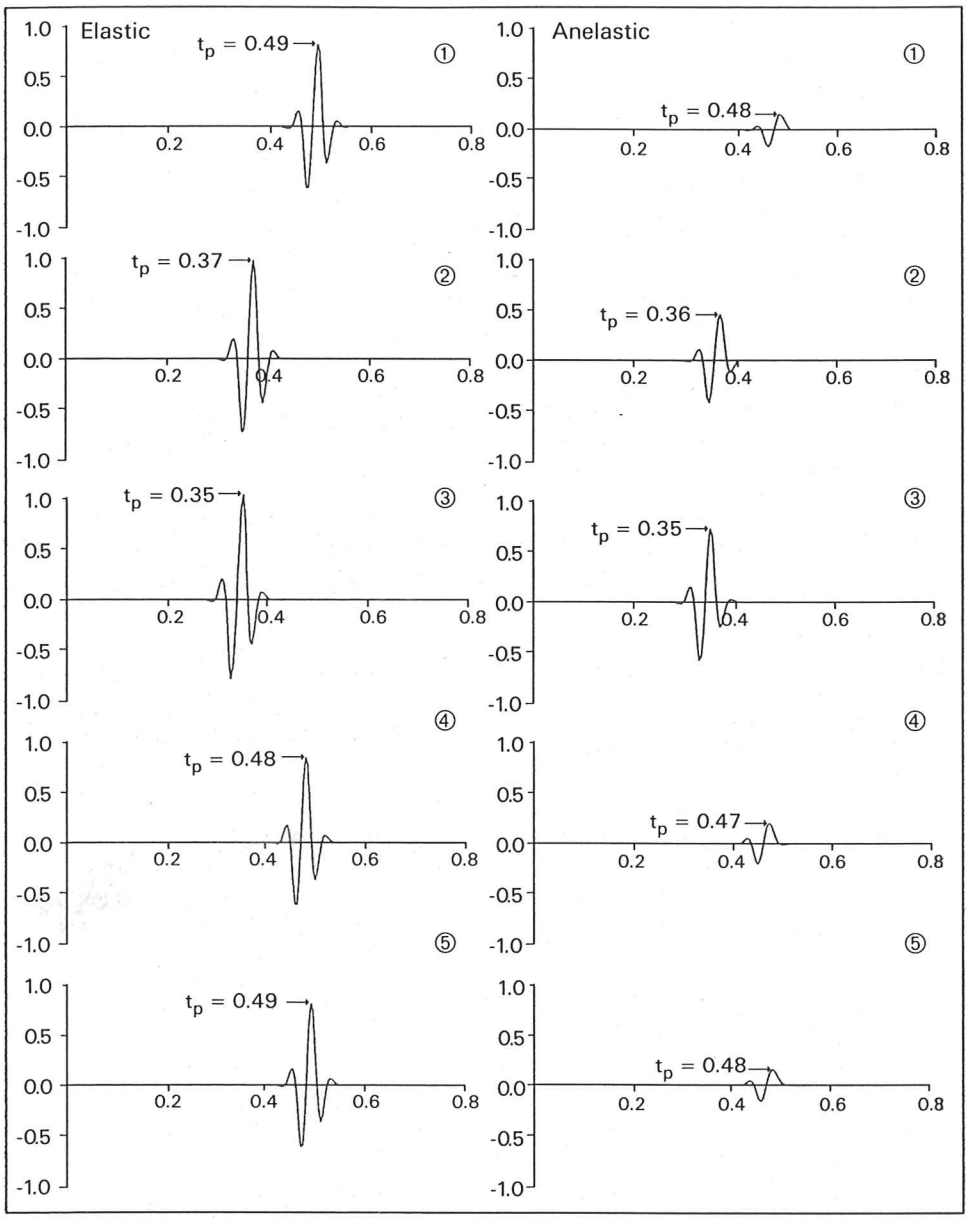

Figure 2. Elastic and anelastic solutions at the five receivers represented in Figure 1. Anisotropy is evident from the different locations of the pulse. The different values t_p at each receiver imply velocity dispersion, and the relative amplitude differences at receivers 1 and 3 reveal the anisotropic attenuation effect.

To illustrate the anisotropy and dispersion effects, we represent in Figure 1 the position of the positive peak at 0.7s propagation time. The black and empty dots are the elastic and anelastic cases, respectively. These positions are computed with velocity information taken from Figure 2, i.e., dividing 800m by the respective t_p. For the elastic case, this velocity should be close to the group and energy velocities (in elastic media they coincide). In the anelastic medium, the wavefront constructed with the empty dots should resemble the wavefront defined by the energy velocity (i.e., velocity times one unit of propagation time) [5]

Finally, it is clear from Figure 2 that the pulse travelling in the vertical direction (receiver 1) has been attenuated more than the pulse travelling in the horizontal direction (receiver 3). This is in agreement with the previous choice of quality factors. It can be shown [5] that the attenuation curve for homogeneous viscoelastic plane waves gives a higher value in the direction of receiver 4 than in the direction of receiver 2. This fact explains the asymmetric dissipation around the x-axis.

We show in another article [6] that (15) gives also the magnetic field of TEM (transverse electric and magnetic) waves propagating in a conducting monoclinic medium, provided that the compliance matrix $\mathbf{p}^{-1}$ is replaced by a complex dielectric matrix and that the density is replaced by the magnetic permeability. The present solution is useful to study the physics of wave propagation in terms of the stiffnesses and anelastic properties of real materials at any frequency band. In addition, the solution serves as a test for acoustic and electromagnetic simulation codes.

Acknowledgements

This work was supported in part by the Commission of the European Communities under the JOULE project.

References

[1] Schoenberg, M. and Costa, J., ***The insensitivity of reflected SH waves to anisotropy in an underlying layered medium,*** *Geophys. Prosp.*, **39,** 985– 1003, (1991).

[2] Ben-Menahem A. and Singh, S.G. ***Seismic Waves and Sources,*** Springer Verlag, New York, (1981).

[3] Auld, B. A., ***Acoustic Fields and Waves in Solids, Vol.I,*** Robert E. Krieger, Publishing Co., Malabar, Florida, (1990)

[4] Morse, P.M. and Feshbach, H., ***Methods of Theoretical Physics,*** McGraw-Hill, New-York, (1953).

[5] Carcione, J. M., ***Wavefronts in dissipative anisotropic media,*** *Geophysics,* in press, (1993).

[6] Carcione, J.M., and Cavallini, F., ***On the acoustic-electromagnetic analogy,*** submitted to *Geophysics,* (1993).

(Received 1 October 1993)